Journal of Solution Chemistry (2024) 53:80–90
https://doi.org/10.1007/s10953-023-01268-1

The Curious Case of 1-Ethylpyridinium Triflate: Ionic Liquid Exhibiting the Mpemba Effect

Mirosław Chorążewski[1] · Michał Wasiak[2] · Alexander V. Sychev[3] · Vadim I. Korotkovskii[3] · Eugene B. Postnikov[4]

Received: 29 November 2022 / Accepted: 19 February 2023 / Published online: 1 April 2023

Abstract
Here, we report the results of qualitative and quantitative investigations of the first-order phase transition in the ionic liquid 1-ethylpyridinium triflate exhibiting a high variability of temperature ranges, within which the freezing and melting occur. By two methods, the direct fast quenching/annealing and the slow temperature-controlled differential scanning calorimeter, it is revealed that despite the almost constant absolute enthalpies of phase transition, the freezing occurs faster with the larger temperature contrast (cooling rate) between the initially hotter sample and the colder surrounding. This feature is a clear exhibition of the Mpemba effect. The regularity in the change of the melting point is analyzed as well.

Keywords Ionic liquid · Mpemba effect · Dynamic calorimetry · First-order phase transition · Metastability

1 Introduction

This work is dedicated to the memory of Professor Jean-Pierre E. Grolier. He was one of the pioneers of the modern calorimetry, especially *scanning transitiometry* [1]. Among many scientific interests, Professor Grolier investigated liquid–solid equilibria [2] and phase transitions in polymers [3, 4]. His work was inspiration to many scientists.

Modern dynamic lifestyles coupled with an increase in renewable energy penetration in the power production mix have resulted in an increased supply–demand intermittency issue

✉ Mirosław Chorążewski
miroslaw.chorazewski@us.edu.pl

✉ Eugene B. Postnikov
postnikov@kursksu.ru

[1] Insititute of Chemistry, University of Silesia in Katowice, Szkolna 9, 40-006 Katowice, Poland

[2] Department of Physical Chemistry, University of Łódź, ul. Pomorska 165, 90-236 Łódź, Poland

[3] Laboratory of Molecular Acoustics, Kursk State University, Radishcheva St., 33, 305000 Kursk, Russia

[4] Department of Theoretical Physics, Kursk State University, Radishcheva St., 33, 305000 Kursk, Russia

[5]. This issue can be resolved through low-cost energy storage technologies [6]. Thermal energy storage (TES) is such a technology [7]. Latent heat storage (LHTES) is currently the most promising TES sub-category with rapidly increasing scientific output and recently reported industrial applications in solar energy and waste heat recovery. LHTES is based on the ability of a material, commonly referred to as the phase change material (PCM), to absorb/release heat isothermally during its transition from one state to another (most commonly solid to liquid). Among several PCMs, ionic liquids are promising candidates for LHTES applications owing to their small volume change during phase transition, flexible design, high heat of fusion, good thermal stability, low flammability, and low toxicity [8]. Shi et al. recently propose a computer-aided molecular design (CAMD)-based method to systematically design IL PCMs for a practical TES process [9]. Zhang et al. fabricated tubular carbon fiber-ionic liquids/stearic acid (CF-ILs/SA) composite phase change materials and reported good thermal conductivity and storage capacity. An extensive literature review on applications of ionic liquids in TES has been recently published by Piper et al. [10]. Among the possible PCM applications, a particular problem is the consideration of suitable materials for cooling and cold-chain transportation systems, for which a variety of materials with high latent heat cannot be used due to their high freezing/melting temperatures.

Sanchez et al. [11] investigated the physicochemical properties of 1-ethylpyridinium triflate as well as its aqueous solutions, with a view to its use for absorption heat pumps. This type of study requires knowledge not only of the basic physicochemical quantities, but also a full characterization of the phase transitions that occur, together with determination of the liquidity range of potential ionic liquids as absorbents for refrigerants.

There is a quite limited set of experimental data obtained from direct measurements of thermodynamic properties of 1-ethylpyridinium triflate. The authors of the work, which discussed phase transitions in series of ionic liquids [12], by means of the DSC with the cooling rate 5 °C·min^{-1} and the heating rate 10 °C·min^{-1} determined two exothermic peaks (–16 and –10 °C) during cooling and two endothermic (– 7 and 32 °C) peaks during heating. In the work [11], the density and the viscosity of this IL were measured at atmospheric pressure in the temperature range (293.15–353.15) K. Although its lower limit is slightly below the largest melting temperature mentioned above, it exceeds the expected crystallization temperature. Therefore, when the IL was taken in the liquid state, it is not surprising that it kept this state while heated. This route is explicitly reported in the more comprehensive work [13], where a variety of thermodynamic properties was studied within the range (293.15–338.15) K; it has been noted that the liquid was heated up to $T = 323$ K to obtain the liquid state. It should be pointed out that in contrast to the work [12], the DSC measurements with the cooling/heating rates 10 °C·min^{-1} did not reveal an onset of crystallization down to 262.5 K, i.e., – 10.65 °C, which coincides with the lowest peak from the work [12]. But existence of the liquid state up to such low temperatures provided the reason why the Ionic Liquids Database—ILThermo (v2.0) (https://ilthermo.boulder.nist.gov/) supplied all these data with the comment "Metastable liquid." Surprisingly the melting was detected with the onset at 289 K and the peak at 300.4 K (15.85–27.25 °C). To the best of our knowledge, there are no other data reported in the literature. However, it also should be pointed out that the commercially available samples of 1-ethylpyridinium triflate exist in the solid state when kept at room temperature for a sufficiently long time that means that their crystallization temperature should be higher that the value reported in the literature.

It should be pointed out that the effect of the dependence of the crystallization and melting temperatures on the cooling/heating rate was previously detected for different kinds of pure ionic liquids [14–16] and, in particular, discussed as connected to multistep phase

transitions [17] originated from a possible variety of microscopic structural ordering. The latter problem is directly in line with the modern fundamental interest to the complex interplay of chemical and physical properties of constituents of ionic liquids reflected in their phase transition properties [18].

On the other hand, the peculiar behavior of the freezing at the different temperature conditions can be related to the so-called Mpemba effect. The Mpemba effect was originally noted [19] as a phenomenon of faster freezing of hot water in comparison with the cool one. Despite numerous studies, its origin and conditions of emerging are still unclear and controversial topics in the case of water, see e.g., [20–22]. At the same time, this effect in the general sense of a faster occurrence of the solidification phase transition when a system was prepared in initially hotter state than in cooled one, gains an active recent attention within the context of non-equilibrium statistical physics and thermodynamics [23]. An existence of the Mpemba effect was confirmed in crystallization of quenched polymer melts [24], colloids [25], granular fluids, and active particles [26, 27]. The theoretical understanding of these generality addresses metastability of such systems when initial heating may allow simplified transitions between multiple possible local minima in the energy landscape [28–30].

Thus, the principal goal of this work is to explore the phase transitions (freezing and melting) in 1-ethylpyridinium triflate by varying conditions leading to the phase change in a wide range and analyzing the respective response.

2 Materials and Methods

The ionic liquid, 1-ethylpyridinium triflate (ethylpyridinium trifluoromethanesulfonate, [EtPy][OTf], the chemical formula $C_8H_{10}F_3NO_3S$), was purchased from the company IoLiTec GmbH (Germany). When purchased, at the room temperature, the substance was in the solid form. It was heated up until melted, and then the sample was kept at 90 °C at vacuum for about 24 h. The purity declared by manufacturer was 99%. Water content in the sample was determined by volumetric Karl–Fischer titration using Schott Instruments GmbH TitroLine KF Titrator. The maximum content of the water was determined not to exceed 0.00035 mass fraction units.

Within this investigation, two sets of approaches were used: (i) the quenching applied to relatively large volumes of the ionic liquid sample realized as the movement of the IL-filled vessel equilibrated in the temperature with a thermostat maintaining a high temperature to another thermostat with a low temperature and, after cooling, back; tracing the change of temperature indicating phase transitions are close as the experimental route to the original method for revealing the Mpemba effect [19] and (ii) more detailed quantitative investigation via the differential scanning calorimetry of small samples with the preciously controlled temperature and heat flows.

2.1 Quenching

Experiments for the quenched freezing and melting were carried out using the thermostat KRIOVIST-03 (Termex Russia) as a cooling reservoir and the thermostat VIS-T-02, (Termex Russia) as a heating reservoir. The experimental procedure was organized as follows: 2.5 ml of the ionic liquid in a hot liquid state was added to a pycnometer having the total volume of 5 ml and the 1000 Ω platinum resistance thermometer was also placed inside of

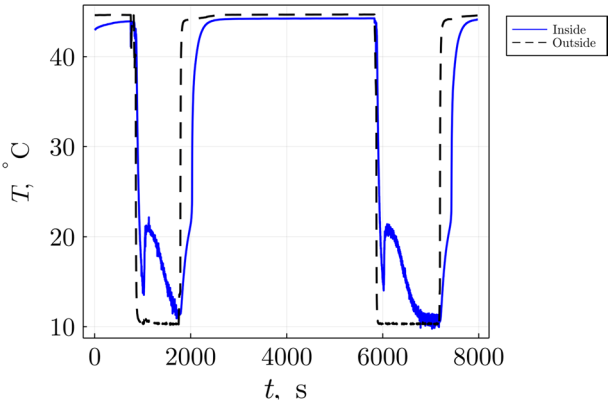

Fig. 1 An example of thermograms recorded from the platinum thermometer immersed in 1-ethylpyridinium triflate filling the vessel, which was periodically moved between thermostats with different temperatures, and from the thermometer placed outside the vessel in the fluid filling these thermostats. During the depicted experiment, the sample was initially placed in the thermostat kept at 44 °C and then transferred to thermostat set to 10 °C. Experiment was repeated twice

Table 1 Data of the temperatures of two, hot and cold, thermostats used for the quenching experiments (the numbers correspond to the same in Figs. 2 and 3) and the respective temperatures of phase transitions

Experiment	T_{max} (°C)	T_{min} (°C)	T_f (°C)	T_m (°C)
(I)	49	− 19	31	33
(II)	49	− 7.2	8.2	33
(III)	44	2.2	27	33
(IV)	44	5.6	17	23
(V)	42	7.1	14	23

the vessel. To avoid a current leakage due to ionic liquid's conductivity, the platinum wire was covered by a thin layer of rosin insulation. The second sensor of the same kind was left outside the pycnometer to record accurately the temperature of the surrounding fluid filling the thermostat in the direct vicinity of the experimental vessel. Both thermometers were connected to a digital thermometer bridge (Terkon, Termex Russia) having the standard uncertainty $u(T) = 0.01$ K and the time step of recordings passed to a computer equal to 0.8 s.

During the quenching procedure, the IL-filled vessel was placed into the hot thermostat and kept inside up to the stabilization of the temperature, then it was fast transferred to the cold thermostat and a thermogram of cooling was recorded. After reaching the lowest temperature, the vessel was moved to the hot thermostat and thermogram of heating was recorded up to the complete melting of the IL and equilibration with the surrounding fluids in the thermostat. A typical example of the thermograms for such cycles is shown in Fig. 1. Five experiments with different values of temperature of hot and cold thermostats were performed. Values of the temperature of both hot and cold thermostats in experiments denoted as (I)–(V) are listed in Table 1. The procedure was repeated several times for each pair of high/low temperatures.

2.2 Differential Scanning Calorimetry

To investigate the phase behavior of the 1-ethylpyridinium triflate at different temperature conditions, Setaram (France) micro-DSC III differential scanning calorimeter was used. A "batch"-type cell with volume of about 1 cm^3 was used. In all experiments, a similar

empty cell was used as reference. The mass of the samples was around 10 mg. The calorimeter was factory heat calibrated with the Joule effect, and temperature calibration was performed using two different substances (water, naphthalene) at a few different heating rates as recommended by the manufacturer. Standard uncertainty of the absolute temperature determination was estimated at 0.05 K. Enthalpy accuracy was estimated to be 1%. To preheat the samples, lab oven SLN 53 ECO by POL-EKO was used.

3 Results and Discussion

The results of the macroscopic quenching procedure are illustrated as thermograms shown in Fig. 2. The respective temperatures of freezing (crystallization) and melting are determined from the location of the onsets typical temperature changes in the temperature curves indicating the presence of a phase transition. The freezing phase transition temperature is identified by the point at which the fast temperature elevating jump starts. The melting phase transition is indicated by the kink in the temperature dependence on time. The respective numerical values for all listed experiments are given in Table 1. Despite high irregularity in the freezing points, one can note some trend showing that faster cooling results in faster freezing, i.e., elevation of the freezing temperature, which is in all cases significantly larger than in the DSC-based experiments with slow cooling. Interestingly that the highest detected freezing temperature (31 °C) is not much different from the highest meting temperature (33 °C). This case corresponds with the maximal contrast of temperatures between the hot and cold thermostats (68 °C, experiment (I)). We can hypothesize that this coincidence originates from the absence of de-jamming of particles arranging in the solid state due to the heat to the heat released during crystallization. Figure 3 explicitly illustrates both the onset time of freezing after the placing the vessel with the heated IL into the cold thermostat and the time which takes to freeze the sample as a function of difference in temperature between two thermostats. As it is seen in Fig. 3, the respective

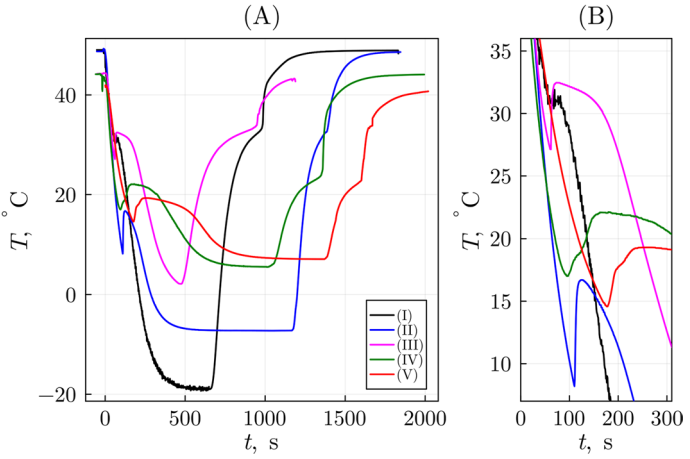

Fig. 2 Thermograms for quenching experiments with different heat exchange rates. The experimental conditions denoted in the legend by Roman numerals are listed under the same numbers in Table 1. The subpanel (**A**) illustrates the full one cooling/heating cycle for each condition, and the subpanel (**B**) is an enlarged part of the plot around the freezing phase transition

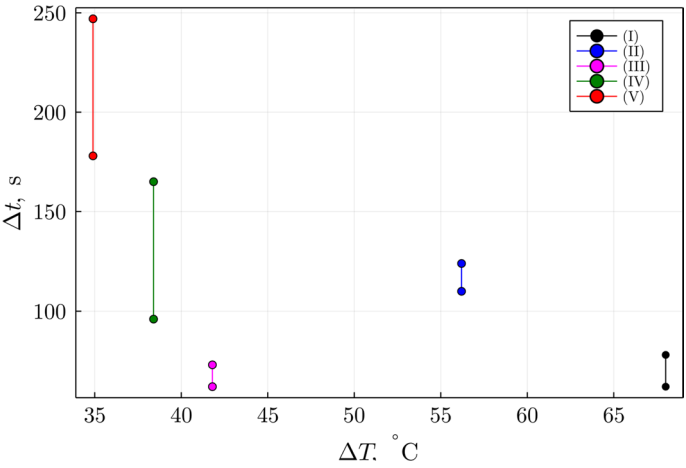

Fig. 3 The dependence of time left from the start of quenched cooling (zero time in Fig. 2A) to the freezing for different temperature differences of the sample and the thermostat. Each lower circle denotes the starting point of the phase transition (the time moment corresponding to the local minimum extreme point in Fig. 2B) and the upper one marks the time of reaching local exothermic maximum in the temperature curve in Fig. 2B. Roman numerals in the legend correspond to the experiments listed under the same numbers in Table 1

temperature jump for the curve (I) is quite small in comparison to other curves. This means that the extremely cold surrounding draws heat away from the IL sample, and the emergence of the crystallization microscopic germs immediately leads to the full solidification practically not disturbed by the exothermic effects of the phase transition destroying the seeds. The same effect is qualitatively visible for the pair of experiments (III) and (IV).

Melting temperatures determined in these experiments are more stable with respect to the temperature difference between thermostats, only two different values were detected, (33 °C) and (23 °C). Notably that the later value is detected for two [experiments (III) and (V)] highest starting temperatures of the solid state (note also that freezing temperatures were not greatly higher than melting ones in these cases). This effect can also be considered as arguing in favor of high metastability of 1-ethylpyridinium triflate on the boundary of the first-order phase transition: the microscopic ordering is can be destroyed more easily when it is formed at temperatures nearer to the surrounding ones.

To represent the obtained data in the form allowing the discussion of the Mpemba effect, i.e., a dependence between the temperature contrast and the time interval required for freezing, we plotted this dependence explicitly in Fig. 3 determining the time moments corresponding to the points of local minimum and maximum in the temperature curves and plotting them as a function of the mentioned temperature differences in thermal baths. One can clearly see a qualitative exhibition of the Mpemba effect: the situations of larger temperature contrast between initial state of the ionic liquid and the cold thermostat leads as a rule to the faster freezing. Note that this acceleration cannot be associated only with the faster cooling due to the heat flow gradient because the larger temperature difference results also in the elevated freezing point as seen in Fig. 2 and Table 1. Rather, it looks as a confirmation of the theoretical ideas mentioned above about a metastable character of 1-ethylpyridinium triflate in the vicinity of its solidification. As an additional support of this conclusion, we draw attention to curves (IV) and (V) in Fig. 2 where one can see

non-smooth temperature growth between the transition initiation and the maximal temperature value originated from the exothermic heat release during the freezing. It is in line with the interpretation of metastability as non-equilibrium transitions between multiple local equilibria [30, 31]. These transitions require longer time that is also visible from respective intervals in Fig. 3.

As the next, more quantitative exploration of the revealed effect, the technique of the differential scanning calorimetry was applied.

As the first step, the IL-filled cell preheated in lab oven at 200 °C was introduced to the calorimeter, which was set to isotherm at 0 °C, and then observed under isothermal condition. The main purpose of this experiment was to check whether this ionic liquid can be in a metastable state after fast quenching that may be considered as one of premises of the Mpemba effect. After about 1000 s, the exothermic peak was observed, see Fig. 4, where the initial interval of drastic changes in the heat flows originated from the highly contrast temperature change is omitted and the interval around the phase transition at the stabilized temperature condition is highlighted. The enthalpy of the exothermic effect is equal to − 50.5 $J \cdot g^{-1}$. Thus, we can conclude that metastability is already present in the system and its existence may affect the occurrence of the phase transition when the heat flow is variable but with different rates.

Further, the experimental conditions were changed directly to reproduce Mpemba's experiment but with the precisely controlled change of the heat flow. The controlled slow cooling with different cooling rates was carried out, see Fig. 5. These experiments did not reveal any peaks indicating freezing of 1-ethylpyridinium triflate at 0 °C in contrast to the quenching procedure. However, the scanning from 0 °C down to – 15 °C revealed the freezing phase transitions at lower temperatures, which strongly depend on the rate of the temperature's decrease. The exothermic peaks in this case are much sharper than in the case of quenching and the onset temperature changes from − 3.59 °C down to − 7.30 °C with a decrease of the scanning rate. At the same time, this shift of the freezing temperature is the main difference between two cases, the enthalpy of freezing does not differ significantly (− 61.4 $J \cdot g^{-1}$ and − 62.4 $J \cdot g^{-1}$, respectively).

The subsequent heating of the frozen samples is shown in Fig. 6. During heating on both curves (I) and (II), an endothermic peak, corresponding to the melting process, was observed. With the increase of the scanning rate from 0.3° $C \cdot min^{-1}$. to 0.5 $°C \cdot min^{-1}$, the onset temperature shifts from 16.33 to 15.83 °C. The peak point temperatures are 19.7 °C

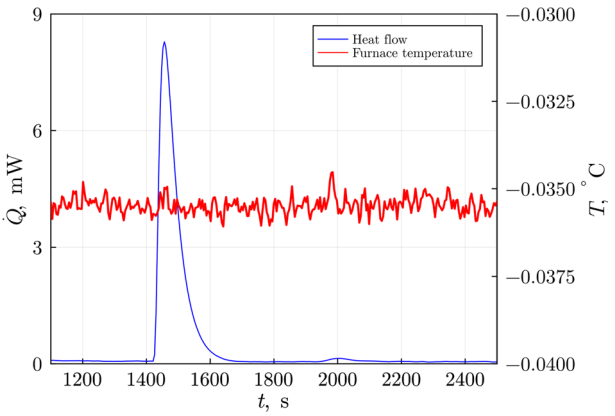

Fig. 4 An example of the heat flow registered with a calorimeter in the long-term isothermal regime (as indicated by the plot of the furnace temperature) observed after from the initial fast precooling of 1-ethylpyridinium triflate sample from 200 °C down to 0 °C. Only the time interval after the furnace temperature stabilization is shown, during of which a spontaneous freezing occurred

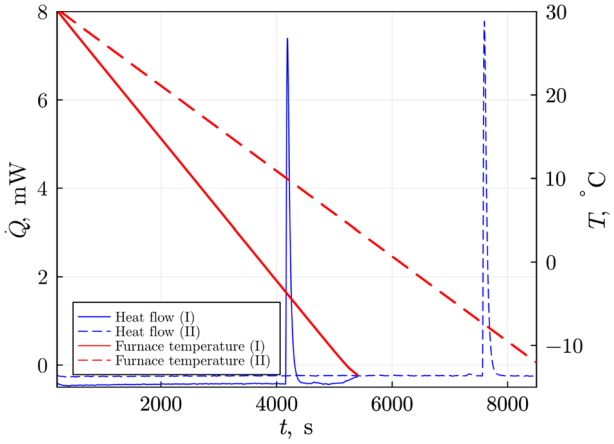

Fig. 5 Heat flows during cooling 1-ethylpyridinium triflate from 30 to − 15 °C at the 0.5 °C·min^{-1} (I) and 0.3 °C·min^{-1} (II) scanning rates, which are explicitly illustrated by the plots of temperature in the furnace implementing this cooling at the same time scale

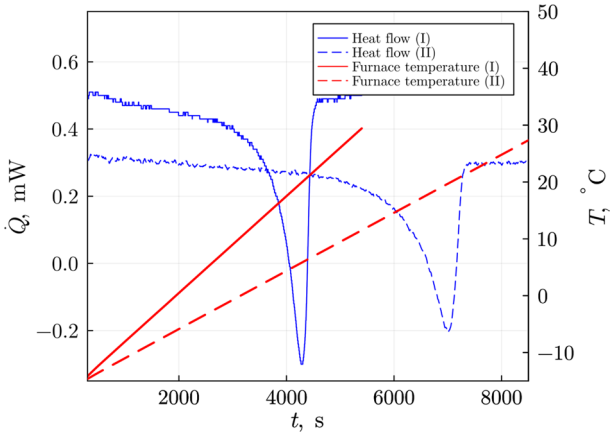

Fig. 6 Heat flows during heating frozen 1-ethylpyridinium triflate from − 15 to 30 °C at the 0.5 °C·min^{-1} (I) and 0.3 °C·min^{-1} (II) scanning rates, which are explicitly illustrated by the plots of temperature in the furnace implementing this heating at the same time scale

and 20.0 °C, respectively. The melting enthalpies are close to each other, 58.9 J·g^{-1} and 60.6 J·g^{-1}. Note that areas of all exo- and endothermic peaks are similar with absolute value around 60 J·g^{-1}. The values obtained in those experiments are close to onset temperature 16 °C and enthalpy of melting 44.71 J·g^{-1} presented by García-Andreu et al. [13] and area of the peak during the quenching in the calorimeter depicted in Fig. 4.

Taking into account the distributed range of the first-order phase transition in this ionic liquid, it is interestingly to compare it to predictive methods, which are under an active development last years. Such methods include usage of descriptors of chemical structure and properties of ions as well as more simple group contributions (GC).

Calculations using the quantitative structure–property relationships (QRST) according to the model, chemical descriptors and software provided in Ref. [32], resulted in the predicted melting point T_{QRST} = 8.55 °C. However, this value corresponds not to the experimentally detected melting temperature but rather a vicinity of the lower limit of freezing temperatures experimentally revealed by the macroscopic quenching procedure.

Another set of approaches addresses contributions of groups consisting ions, separate atoms, and some their typical combinations conventionally used in organic chemistry.

Among the group contribution-based values provided in Refs. [33, 34] for the melting temperatures, $T_{GCM1} = 48.47$ °C, $T_{GCM2} = 65.59$ °C, $T_{GCM1-R} = 39.98$ °C, $T_{hybridGCM} = 33.51$ °C only two last versions of the GC approaches give the values quite close to the melting temperatures obtained by the during the annealing procedure (the largest of two versions obtained in different runs, see Table 1), respectively.

Thus, these experiments confirms that the character of the phase transitions themselves as reflected in the absolute values of enthalpies is universal and specific for intermolecular interactions and structural features of liquid and crystal phases of this ionic liquid. At the same time, the explicit variation of the temperatures of the phase transitions, representing the Mpemba effect, argues in favor of the hypothesis that the path of the phase transitions is in general complicated and may go via jamming in some states, which either lead to simplified continuing of being in another phase state or continuing of slow heat-supported restructuring shifting the final-phase transition temperature.

4 Conclusion

The present work was an attempt to investigate the nature of a non-trivial character of the first-order phase transition in the ionic liquid 1-ethylpyridinium triflate. Since this substance can be observed either in liquid or in solid state at the room range of temperatures, two types of calorimetric experiments we carried out. The first experiment regarding quenching/annealing was carried out under conditions far from thermodynamic equilibrium, while the other was differential scanning calorimetry under conditions close to thermodynamic equilibrium. The results of both types of experiments indicate the clear dependence of the freezing temperature and time required for hot/cool liquid to freeze on the temperature contrast or, equivalently, the cooling rate. Such a behavior can be referenced as an exhibition of the Mpemba effect. Its occurrence in this ionic liquid most probably originates from the high metastability of 1-ethylpyridinium triflate in the vicinity of phase transition. Thus, finally, we can conclude that this further exploration of this substance, e.g., at the level of the microscopic energy landscape, oscillation spectral properties, etc. can provide physicochemical insights into the origin of the Mpemba effect in general.

Author contributions MC proposed the concept, performed experiments, performed data processing, computations, and designed and wrote the manuscript. MW performed experiments, performed data processing, and visualizations, and wrote the manuscript. AVS performed experiments. VIK performed experiments. EBP proposed the concept, performed data processing, computations, and visualizations, and designed and wrote the manuscript. All authors discussed and reviewed the whole manuscript.

Declarations

Competing interests The authors declare no competing interests.

References

1. Randzio, S.L., Grolier, J.-P.E., Quint, J.R.: An isothermal scanning calorimeter controlled by linear pressure variations from 0.1 to 400 MPa. Calibration and comparison with the piezothermal technique. Rev. Sci. Instrum. **65**, 960–965 (1994). https://doi.org/10.1063/1.1144926
2. Bitchikh, K., Meniai, A.-H., Louaer, W., Grolier, J.P.: Experimental and modelling of liquid–solid equilibria. J. Équilib. Phases Proc. (2009). https://doi.org/10.1051/jeep/200900011
3. Grolier, J.-P.E., Dan, F., Boyer, S.A.E., Orlowska, M., Randzio, S.L.: The use of scanning transitiometry to investigate thermodynamic properties of polymeric systems over extended T and p ranges. Int. J. Thermophys. **25**, 297–319 (2004). https://doi.org/10.1023/B:IJOT.0000028469.17288.de
4. Grolier, J.-P.E.: Advanced experimental techniques in polymer thermodynamics. Pure Appl. Chem. **77**, 1297–1315 (2005). https://doi.org/10.1351/pac200577081297
5. YekiniSuberu, M., Wazir Mustafa, M., Bashir, N.: Energy storage systems for renewable energy power sector integration and mitigation of intermittency. Renew. Sustain. Energy Rev. **35**, 499–514 (2014). https://doi.org/10.1016/J.RSER.2014.04.009
6. Zhang, H., Baeyens, J., Cáceres, G., Degrève, J., Lv, Y.: Thermal energy storage: recent developments and practical aspects. Prog. Energy Combust. Sci. **53**, 1–40 (2016). https://doi.org/10.1016/J.PECS.2015.10.003
7. Anagnostopoulos, A., Navarro, M.E., Ding, Y.: Microstructural improvement of solar salt based MgO composites through surface tension/wettability modification with SiO_2 nanoparticles. Solar Energy Mater. Solar Cells. **238**, 111577 (2022). https://doi.org/10.1016/J.SOLMAT.2022.111577
8. Das, L., Rubbi, F., Habib, K., Aslfattahi, N., Saidur, R., Baran Saha, B., Algarni, S., Irshad, K., Alqahtani, T.: State-of-the-art ionic liquid and ionanofluids incorporated with advanced nanomaterials for solar energy applications. J. Mol. Liquids **336**, 116563 (2021). https://doi.org/10.1016/j.molliq.2021.116563
9. Shi, H., Zhang, X., Sundmacher, K., Zhou, T.: Model-based optimal design of phase change ionic liquids for efficient thermal energy storage. Green Energy Environ. **6**, 392–404 (2021). https://doi.org/10.1016/j.gee.2020.12.017
10. Piper, S.L., Kar, M., MacFarlane, D.R., Matuszek, K., Pringle, J.M.: Ionic liquids for renewable thermal energy storage: a perspective. Green Chem. **24**, 102–117 (2022). https://doi.org/10.1039/d1gc03420k
11. Sanchez, P.B., Curras, M.R., Mato, M.M., Salgado, J., García, J.: Density and viscosity study of pyridinium based ionic liquids as potential absorbents for natural refrigerants: experimental and modelling. Fluid Phase Equilib. **405**, 37–45 (2015). https://doi.org/10.1016/j.fluid.2015.06.043
12. Villanueva, M., Parajó, J.J., Sanchez, P.B., García, J., Salgado, J.: Liquid range temperature of ionic liquids as potential working fluids for absorption heat pumps. J. Chem. Thermodyn. **91**, 127–135 (2015). https://doi.org/10.1016/j.jct.2015.07.034
13. García-Andreu, M., Castro, M., Gascon, I., Lafuente, C.: Thermophysical characterization of 1-ethylpyridinium triflate and comparison with similar ionic liquids. J. Chem. Thermodyn. **103**, 395–402 (2016). https://doi.org/10.1016/j.jct.2016.08.038
14. Faria, L.F.O., Matos, J.R., Ribeiro, M.C.C.: Thermal analysis and raman spectra of different phases of the ionic liquid butyltrimethylammonium bis (trifluoromethylsulfonyl) imide. J. Phys. Chem. B **116**, 9238–9245 (2012). https://doi.org/10.1021/jp3051824
15. Calvar, N., Gomez, E., Macedo, E.A., Domínguez, A.: Thermal analysis and heat capacities of pyridinium and imidazolium ionic liquids. Thermochim. Acta **565**, 178–182 (2013). https://doi.org/10.1016/j.tca.2013.05.007
16. Gomez, E., Calvar, N., Domínguez, A., Macedo, E.A.: Thermal behavior and heat capacities of pyrrolidinium-based ionic liquids by DSC. Fluid Phase Equilib. **470**, 51–59 (2018). https://doi.org/10.1016/j.fluid.2018.04.003
17. Abe, H., Kishimura, H.: Multistep phase transition in 1-decyl-3-methylimidazolium nitrate ionic liquid. J. Mol. Liq. **352**, 118695 (2022). https://doi.org/10.1016/j.molliq.2022.118695
18. Tang, C., Wang, Y.: Phase behaviors of ionic liquids attributed to the dual ionic and organic nature. Commun. Theor. Phys. **74**, 097601 (2022). https://doi.org/10.1088/1572-9494/ac7e2a

19. Mpemba, E.B., Osborne, D.G.: Cool? Phys. Educ. **4**, 172–175 (1969). https://doi.org/10.1088/0031-9120/4/3/312
20. Brownridge, J.D.: When does hot water freeze faster then cold water? A search for the Mpemba effect. Am. J. Phys. **79**, 78–84 (2011). https://doi.org/10.1119/1.3490015
21. Burridge, H.C., Linden, P.F.: Questioning the Mpemba effect: hot water does not cool more quickly than cold. Sci. Rep. **6**, 37665 (2016). https://doi.org/10.1038/srep37665
22. Zimmerman, W.B.: In search of a Mpemba effect protocol: some hot water does cool and freeze faster than cold. Chem. Eng. Sci. **247**, 117043 (2022). https://doi.org/10.1016/j.ces.2021.117043
23. Bechhoefer, J., Kumar, A., Chétrite, R.: A fresh understanding of the Mpemba effect. Nat. Rev. Phys. **3**, 534–535 (2021). https://doi.org/10.1038/s42254-021-00349-8
24. Hu, C., Li, J., Huang, S., Li, H., Luo, C., Chen, J., Jiang, S., An, L.: Conformation directed Mpemba effect on polylactide crystallization. Cryst. Growth Des. **18**, 5757–5762 (2018). https://doi.org/10.1021/acs.cgd.8b01250
25. Kumar, A., Bechhoefer, J.: Exponentially faster cooling in a colloidal system. Nature **584**, 64–68 (2020). https://doi.org/10.1038/s41586-020-2560-x
26. Lasanta, A., Reyes, F.V., Prados, A., Santos, A.: When the hotter cools more quickly: Mpemba effect in granular fluids. Phys. Rev. Lett. **119**, 148001 (2017). https://doi.org/10.1103/PhysRevLett.119.148001
27. Schwarzendahl, F.J., Lowen, H.: Anomalous cooling and overcooling of active colloids. Phys. Rev. Lett. **129**, 138002 (2022). https://doi.org/10.1103/PhysRevLett.129.138002
28. Lu, Z., Raz, O.: Nonequilibrium thermodynamics of the Markovian Mpemba effect and its inverse. Proc. Natl. Acad. Sci. USA **114**, 5083–5088 (2017). https://doi.org/10.1073/pnas.170126411
29. Klich, I., Raz, O., Hirschberg, O., Vucelja, M.: Mpemba index and anomalous relaxation. Phys. Rev. X **9**, 021060 (2019). https://doi.org/10.1103/PhysRevX.9.021060
30. Zhang, S., Hou, J.-X.: Theoretical model for the Mpemba effect through the canonical first-order phase transition. Phys. Rev. E **106**, 034131 (2022). https://doi.org/10.1103/PhysRevE.106.034131
31. Yang, Z.-Y., Hou, J.-X.: Mpemba effect of a mean-field system: the phase transition time. Phys. Rev. E **105**, 014119 (2022). https://doi.org/10.1103/PhysRevE.105.014119
32. Paduszynski, K., Klebowski, K., Krolikowska, M.: Predicting melting point of ionic liquids using QSPR approach: literature review and new models. J. Mol. Liq. **344**, 117631 (2021). https://doi.org/10.1016/j.molliq.2021.117631
33. Mital, D.K., Nancarrow, P., Zeinab, S., Jabbar, N.A., Ibrahim, T.H., Khamis, M.I., Taha, A.: Group contribution estimation of ionic liquid melting points: critical evaluation and re-finement of existing models. Molecules **26**, 2454 (2021). https://doi.org/10.3390/molecules26092454
34. Mital, D.K., Nancarrow, P., Ibrahim, T.H., Abdel Jabbar, N., Khamis, M.I.: Ionic liquid melting points: structure-property analysis and new hybrid group contribution model. Ind. Eng. Chem. Res. **61**, 4683–4706 (2022). https://doi.org/10.1021/acs.iecr.1c04292